# Detailed Study of the $O^{16}(\gamma,n)O^{15}$ Reaction*

A. S. PENFOLD† AND B. M. SPICER‡
*Physics Research Laboratory, University of Illinois, Champaign, Illinois*
(Received August 1, 1955)

The yield curve for the $O^{16}(\gamma,n)O^{15}$ reaction has been examined in detail over most of the energy region between 15.6 Mev and 23.2 Mev. Fine structure in the form of sudden changes of slope, or "breaks" had been previously reported by the Saskatchewan group. The existence of these breaks was confirmed, and a number of new breaks have been found. The yield curve was analyzed for cross section in the vicinity of a break at 16.03 Mev, and it was found that the cross section has a resonance shape with a width of 18±5 kev. The yield curve breaks are interpreted as manifestations of narrow resonances in the cross section. Integrated cross sections, peak heights, and radiative widths were estimated for all the levels found. On the basis of the radiative widths, it is concluded that, below about 19 Mev the reaction proceeds by absorption of $E2$ radiation, while between 22 and 23 Mev it proceeds principally by absorption of $E1$ radiation. No conclusion could be drawn for the 20 to 21 Mev region. From a consideration of the total integrated cross section, and the cross section at 17.63 Mev it is concluded that the bulk of the gamma-ray absorption by $O^{16}$ takes place into narrow levels.

## INTRODUCTION

THE gross features of the cross section for the $O^{16}(\gamma,n)O^{15}$ reaction have been known for some time. The cross section is small and slowly rising for the first three Mev above threshold, and then, starting at about 19 Mev it increases sharply as the peak of the giant resonance is approached.[1–3] These results represent the gross behavior with detail one and a half Mev or less in extent averaged over. There are two reasons for this averaging. First, the cross-section analyses were made in 1-Mev steps and second, either the yield curve was smoothed before analysis,[1,2,4] or the results were smoothed after analysis.[3]

Early in 1952, workers at the University of Saskatchewan observed a number of abrupt changes of slope in the yield curve of the $O^{16}$ reaction.[5] These abrupt changes of slope will henceforth be referred to as "breaks" or "fine structure." The Saskatchewan group observed five such breaks between the reaction threshold (15.60 Mev) and 17.5 Mev. Further work showed that there were similar breaks in the yield curves for other light nuclei, and that they occurred at different energies in different nuclei. The breaks were interpreted as manifestations of narrow resonances in the total absorption cross section, in analogy with the earlier results of the Notre Dame group[6] on the excitation of low-lying levels with x-rays.

The present paper reports on a detailed study of the $O^{16}(\gamma,n)$ yield curve over most of the energy region between the threshold and the peak of the giant resonance. The purpose of making these masurements was twofold. First, an independent verification of the yield curve breaks reported by the Saskatchewan group was desired, and second, it was planned to obtain as complete a picture of the reaction as possible. Gross measurements[1–3] have indicated a cross section of unusual shape, and the suggestion was made[1] that gamma radiation of more than one multipolarity is involved. It was hoped that this suggestion could be checked if the specific properties of some of the levels responsible for the yield curve breaks could be determined.

## EXPERIMENTAL DETAILS

The very nature of the experiment demanded the maximum control of all factors, so that fine detail in the yield curve could be observed. Consequently, a detailed discussion of the experimental arrangement and procedure will be given.

### (a) Samples

The "oxygen" samples used were hollow cylinders of boric acid ($H_3BO_3$) of mass 61.3 grams, internal diameter 2.06 cm, external diameter 3.40 cm, and length 7.70 cm. They were made by compressing boric acid in a mold under a pressure of ten tons per square inch.

In all, some sixty cylinders were made and counting tests showed that they were identical to within 0.5%. It should be noted that the walls of the cylinders were thick enough so that the counters were not sensitive to the activity near the outer surface, and that the samples more than covered the sensitive volume of the counters. This was important as the cylinders became rather worn after long use.

The samples were bound together in groups of two and groups of four, and were irradiated six at a time. Repeated tests failed to reveal any buildup of long-lived activities due to impurities in the boric acid.

* Supported in part by the joint program of the Office of Naval Research and the U. S. Atomic Energy Commission.

† Present Address, Institute for Nuclear Studies, University of Chicago, Chicago, Illinois.

‡ Fulbright Fellow, on leave from the Physics Department, University of Melbourne, Melbourne, Australia. Present address at the University of Melbourne.

[1] Horsley, Haslam, and Johns, Can. J. Phys. **30**, 159 (1952).
[2] R. Montalbetti and L. Katz, Can. J. Phys. **31**, 798 (1953).
[3] Ferguson, Halpern, Nathans, and Yergin, Phys. Rev. **95**, 776 (1954).
[4] L. Katz and A. G. W. Cameron, Can J. Phys. **29**, 518 (1951).
[5] Haslam, Katz, Horsley, Cameron, and Montalbetti, Phys. Rev. **87**, 196(A) (1952).
[6] E. Guth, Phys. Rev. **59**, 325 (1941), and references given there.

### (b) Counting System

The 2-minute $\beta^+$ activity induced in the samples was counted with thin-walled aluminum Geiger counters (Victoreen thyrode—*IB*85) mounted in nests of two and four in cylindrical lead castles. The boric acid cylinders fitted snugly over the counters.

The stability of the counters was checked frequently with a uranium oxide source pushed onto a rod along the axis of each lead castle. A stability of 0.75% was demanded. It was observed that the counters could be stable to better than 0.75% for long periods of time.

A timing circuit turned the scalers on about 55 seconds after irradiation and off about 210 seconds later. The exact times were read from clocks and a correction was applied to the total count to normalize to a 55- to 210-second scheme. This correction was obtained graphically and it rarely exceeded 1%. The counting system was well removed from the betatron, so that counting could be done while an irradiation was in progress.

### (c) Irradiation Geometry

The source of photons in this experiment was the University of Illinois 22-Mev betatron, and the samples were usually located at 58 cm or 97 cm from the x-ray target.

The boric acid samples and the x-ray monitor were mounted together on an optical bench so as to move as a unit. In this way, the distance between the x-ray target and the sample could be changed without disturbing the geometry. No collimation was used.

The monitor was placed behind the samples in such a way that the x-ray shadow cast by the samples almost exactly covered the sensitive plate of the monitor. Without this "eclipsing" geometry, a slight swinging of the x-ray beam could generate a fictitious break in the yield curve.

### (d) Monitor

The x-ray beam was monitored with an aluminum-walled ion chamber placed behind a two-inch lead brick. The lead brick was used to reduce the sensitivity of the ion chamber and to eliminate possible troubles from ion recombination.

The ion chamber was connected to a vibrating reed electrometer, and a two-minute time constant was introduced into the circuit so that during an irradiation, the dose recorded by the ion chamber was proportional to the activity in the samples. The proportionality was checked experimentally by purposely varying the yield rate from the betatron during an irradiation. The activity per unit dose was found to be independent of fluctuations in the x-ray intensity, even if the fluctuations were very violent. The success of this experiment was due in large measure to the use of the time constant in the monitor circuit.

Temperature and pressure corrections to the monitor response were made after each irradiation.

The energy response of the monitor was determined by reference to that of a "Lucite" monitor (a Victoreen thimble behind four centimeters of Lucite) placed at the position of the samples. The ratio of the response of the ion chamber monitor to that of the "Lucite" monitor was observed to be constant to within 1% in the energy range 12 to 24 Mev.

### (e) Energy Calibration and Stability

The primary energy calibration of the betatron integrator (energy-controlling device) was made by measuring the thresholds for several photonuclear reactions whose threshold energies are known from mass data. The reactions used were $Be^9(\gamma,n)Be^8$, $O^{16}(\gamma,n)O^{15}$, $C^{12}(\gamma,n)C^{11}$, and $Cu^{63}(\gamma,n)Cu^{62}$ with thresholds of $1.664\pm0.002$ Mev,[7] $15.61\pm0.01$ Mev,[7] $18.73\pm0.03$ Mev,[7] and $10.73\pm0.05$ Mev,[8] respectively. This latter value was obtained from unpublished work by the Saskatoon group in which the $Cu^{63}(\gamma,n)$ threshold was compared to the known thresholds of the $N^{14}(\gamma,n)N^{13}$ and $F^{19}(\gamma,n)F^{18}$ reactions.

The integrator dial was tested with a Leeds and Northrup potentiometer and it was concluded that local nonlinearities and backlash were equivalent to 3 kev, at most, and were usually less than this.

A secondary energy calibration system was established for checking on day-to-day fluctuations in the betatron energy[9] and a "standard counting" system was established for monitoring hour-to-hour fluctuations in energy. This standard counting system is described in Sec. (f) below.

The integrator circuits were left on 24 hours a day during any running period.

The betatron was repeatedly observed to be stable to better then 3 kev for periods of several hours at a time. The maximum energy fluctuation observed between January, 1954 and June, 1955 was 40 kev. Further details on the energy stability of the betatron are given elsewhere.[9]

### (f) Standard Counting

Hour-to-hour drifts in energy can be monitored by using a point on the yield curve where the activity per unit dose induced in the sample is known for a given integrator setting. At this integrator setting, the activity should increase rapidly enough so that small variations in energy can be detected.

It was observed that the slope of the yield curve at about 17.3 Mev (integrator setting 7-030) was large enough so that the yield changed by 2.3% per 6-kev change in energy. Counting statistics at this point were 0.7% so that energy shifts of less than 3 kev could be detected. Standard counting at an integrator setting

[7] F. Ajzenberg and T. Lauritsen, Revs. Modern Phys. **27**, 77 (1955).

[8] Robinson, McPherson, Greenberg, Katz, and Haslam (unpublished).

[9] B. M. Spicer and A. S. Penfold, Rev. Sci. Instr. **26**, 952 (1955).

of 7-030 was chosen as the means of monitoring short-term energy fluctuations. About 25% of the working time was spent in standard counting, in order to keep a close check on the energy.

### PROCEDURE IN TAKING DATA

The boric acid samples were irradiated in the betatron beam for from $2\frac{1}{2}$ to 3 minutes, depending on the energy.

The pole bolt temperature of the betatron was maintained constant by keeping the magnet excitation on continuously during the fifteen-hour day, except for a shutdown of about one minute at the end of each run. In hot weather, the shutdown time was increased somewhat.

A daily routine was established after a period of trial and error, and then was strictly adhered to. A one-hour warm-up time was allowed each morning before any attempt was made to take data. During this time the counter stability was checked with the uranium oxide source. Then a series of irradiations was done at integrator setting 7-030 to examine the energy stability. When it was observed that the betatron was stable to about $\pm 3$ kev, irradiations for the accumulation of data would begin. Thereafter, one irradiation in four to six was done at integrator setting 7-030.

The $O^{16}(\gamma,n)O^{15}$ yield curve was examined in sections about 0.5 Mev in extent. The chosen region was first bracketed with two irradiations. Points were then taken every 60 kev working monotonically up the curve, and then every 60 kev working monotonically down the curve, in such a way that there was a point every 30 kev. After that, data would be taken at randomly chosen energies until there was a point every 6 or 12 kev. In this way the generation of breaks due to systematic errors was avoided.

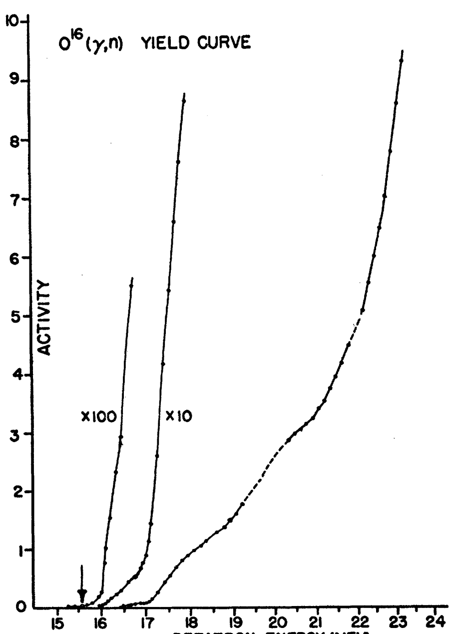


FIG. 1. Over-all yield curve for the $O^{16}(\gamma,n)O^{15}$ reaction, constructed from the detailed measurements described.

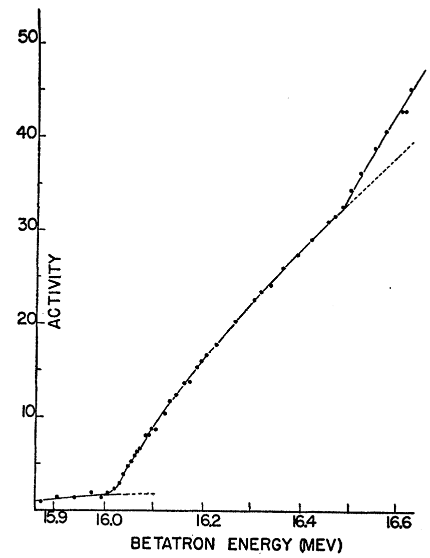


FIG. 2. Yield curve between 15.9 Mev and 16.6 Mev.

Energy shifts indicated by the standard counting were applied to the data as they were taken, as were temperature and pressure corrections to the monitor response.

### RESULTS

As mentioned, the yield curve was examined in small sections—about 0.5 Mev at a time. To set an over-all picture of the curve, the results of sectional measurements were combined to give the curve shown in Fig. 1. The points plotted there do not represent experimental measurements, but were taken from a curve drawn through the data. No data were taken in the regions shown by dotted lines.

It is of interest to compare the yield curve of Fig. 1 with these published by Katz *et al.*[10] There is very good general agreement between the over-all shape of the present curve and those published by Katz. The energy assignments agree up to about 17.5 Mev but disagree at higher energies. The difference may be traced to the difficulty of measuring the $C^{12}(\gamma,n)C^{11}$ threshold for the energy calibration. For this work, a very careful measurement of the carbon threshold was made, and it was discovered that the first break in the $C^{12}(\gamma,n)$ yield curve had been mistaken for the threshold in our previous measurements of it. There is good reason to believe that this mistake had been made in all previous calibrations at Illinois, and that the error is not confined to this laboratory. A more detailed discussion of the measurement of this threshold is given elsewhere.[11]

Some of the detailed results obtained in this experiment are shown in Figs. 2 to 5.

Figure 2 shows the yield curve in the region of the threshold (15.61 Mev), and the data represent 24 hours of working time. The points shown are the averages of

[10] Katz, Haslam, Horsley, Cameron, and Montalbetti, Phys. Rev. **95**, 464 (1954).
[11] B. M. Spicer and A. S. Penfold, preceding paper [Phys. Rev. **100**, 1375 (1955)].

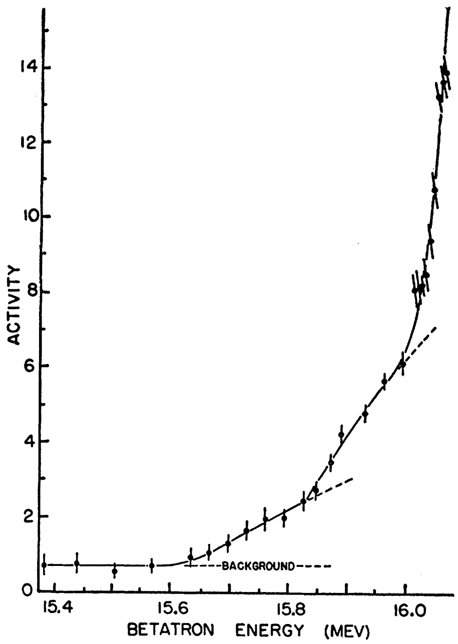


FIG. 3. Yield curve between threshold and 16.1 Mev.

from two to four irradiations. Two decidedly abrupt changes in slope (breaks) are evident in the figure, and the region between the breaks is concave downward. This is consistent with the idea that the yield curve for a narrow resonance should approximate the shape of an isochromat of the bremsstrahlung spectrum.

Both of the breaks in Fig. 2 were reported by Katz *et al.*,[10] but the region between the breaks was reported to be straight. This conclusion could easily be reached if points are taken at 50-kev intervals. It is clear from Fig. 2 that if data were taken every 50 kev or so, and if the curve was not carefully followed near 16 Mev, the energy assigned to the 16-Mev break could be as low as 15.93 Mev.

The portion of the yield curve between 16.0 Mev and threshold is only poorly determined in Fig. 2. An attempt was made to examine this region in more detail. To do this, groups of cylindrical samples were moved up to about 20 cm from the betatron target so as to increase the yield. The results are shown in Fig. 3.

The experimental points which are shown in Fig. 3 were obtained by averaging the results of from two to four irradiations. The break shown at 15.83 Mev is a very weak one and is previously unreported. The shape of the yield curve right near the threshold is not well determined, due to the relatively large statistical error on the measurements, but one can conclude that there is probably a level in the near vicinity of threshold. Barrier effects may strongly affect the shape of the curve near threshold.

Figure 4 shows the yield curve between 16.75 Mev and 17.08 Mev. This is the region immediately above that shown in Fig. 2. The two sets of data are plotted as they were taken—without any normalization—and the figure shows the excellent day-to-day reproducibility which was obtained. Breaks occur at 16.95 and 17.02 Mev. A further break was observed at 16.75 Mev. This comes at the left hand edge of Fig. 4 and is not shown. Katz *et al.*[10] report breaks at 16.7 and 16.9 Mev. The latter is probably an average over the two breaks shown in Fig. 4. It is clear from the figure that data have to be obtained in very closely spaced intervals in order to resolve the two breaks. Representative statistical errors are shown on two of the points in Fig. 4.

The break reported at 17.1 Mev by Katz *et al.*[10] was resolved into two breaks, one at 17.13 Mev and the other at 17.18 Mev. The sample to x-ray target distance used was 97 cm. When this distance was decreased to 68 cm the two breaks could not longer be resolved owing, presumably, to the increased thick target effects. A single, rather rounded break was then observed at an energy of 17.15 Mev.

Three previously unreported breaks were found at energies of 17.55, 17.68, and 17.84 Mev. In this region the breaks are much harder to detect. As one proceeds up the yield curve, breaks of a given but constant strength become more and more difficult to detect since the percentage change in activity which they occasion becomes smaller and smaller. The statistical error cannot be made smaller than about 0.7% per irradiation because of counter jamming during the initial part of the counting interval.

To gain confidence in the ability of the experiment to resolve the small breaks, a type of Monte Carlo game was played. This game operated as follows. Two players, *A* and *B*, begin by establishing a prearranged ordinate and abscissa scale on two sheets of graph paper. The players then separate and *A* draws a yield curve on his graph paper. This curve has the same general slope as the experimental curve, and may have breaks in it

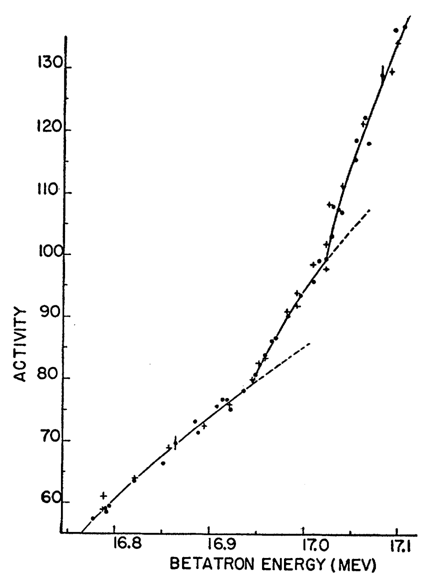


FIG. 4. Yield curve from 16.75 Mev to 17.1 Mev. The dots and crosses represent two different runs.

or not at $A$'s discretion. Player $B$ is the "experimenter" and he makes a yield curve measurement by calling out an energy to $A$. The latter reads the yield curve value at this energy from his graph, applies a statistical error to it and calls out the result. $B$ then plots the point on his graph. In this way a "measurement" is made. To assign a statistical error to the yield curve value, $A$ makes use of a box of numbers distributed about unity with 1% standard deviation. Player $B$ continues to make "measurements" until he is quite sure of the nature of his yield curve. In making the measurements, he attempts to adhere as closely as possible to the attitude which was adopted in the real experiment. When $B$ is satisfied he terminates the measurements and $A$ and $B$ compare curves.

The results of the Monte Carlo games which were played were most gratifying. About twenty different games were played, and in all cases the breaks were detected and their energy was correctly determined. Further, in no case was nonexistent structure read into the curves. In fact, structure weaker than was actually observed could be resolved if the fluctuations of points were entirely due to statistics and not to other experimental difficulties.

Figure 5 shows the yield curve between 21.1 and 21.7 Mev. The breaks in the yield curve are still clearly evident. The breaks shown here are about an order of magnitude stronger than those shown in Fig. 4. The region covered by this figure is on the rising portion of the giant resonance of the $O^{16}(\gamma,n)O^{15}$ cross section[1–3]. Four breaks were also found between 22.3 and 23.2 Mev. These energies are near the peak of the giant resonance.

## ANALYSIS OF DATA AND RESULTS

### (a) The Cross Section near 16 Mev

An analysis of the yield curve was made in the vicinity of the 16.03-Mev break in an attempt to determine the shape of the cross section responsible for the break. The portion of the yield curve below 16 Mev was

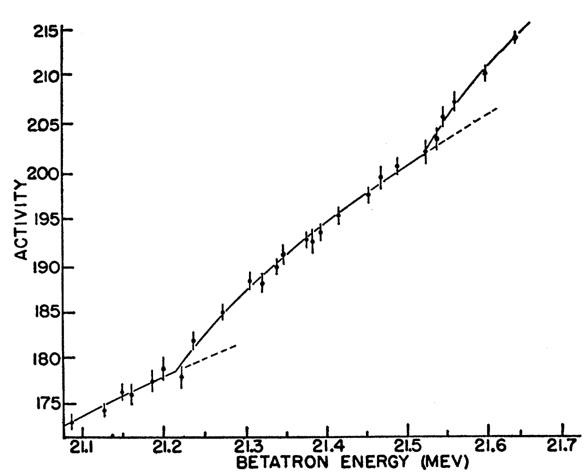


FIG. 5. Yield curve from 21.1 Mev to 21.7 Mev.

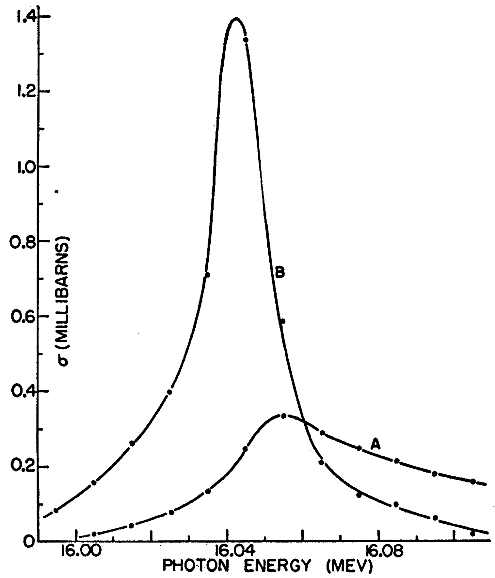


FIG. 6. Cross section near the 16.03 Mev break. Curve $A$ is the cross section obtained by using a thin-target spectrum. Curve $B$ is the cross section after correcting for thick-target effects.

extrapolated smoothly to higher energies and subtracted off the total yield. In this way, the yield due to the level near 16 Mev was obtained. A smooth curve was drawn through the result, and it was analyzed for the cross section by the photon difference method[4,12] in 10-kev steps. The analysis was based on the integrated-over-angle bremsstrahlung cross section derived by Schiff[13] and curve $A$ of Fig. 6 shows the result.

The cross section rises rather sharply on the low-energy side, but falls off more slowly on the high-energy side. The high-energy tail actually extends for several hundred kilovolts.

A correction was made for thick-target effects according to the method of Penfold and Leiss[12] and the result is shown as curve $B$ in Fig. 6. This correction takes account of multiple scattering and energy loss of the electrons in the radiator, energy straggling associated with ionizing or radiative collisions in the radiator, and the intrinsic angular distribution of the bremsstrahlung. The corrected cross section is nearly symmetric in shape, and has a full width at half-maximum of about 18 kev.

An attempt was made to see what features of the cross-section solution were essentially independent of the exact way in which the yield curve was drawn. To do this, a series of smooth curves were drawn through the measured yield curve values, and a cross-section analysis was made for each. All of the curves were kept within the bounds prescribed by statistical errors. It was found that the cross section could be made somewhat asymmetric, but that the width was nearly independent of the yield curve variations.

[12] A. S. Penfold and J. E. Leiss (to be published).
[13] L. I. Schiff, Phys. Rev. 83, 252 (1951).

So far no account has been taken of the energy spread of the electrons striking the radiator, or of energy jitter in the betatron. No exact figures are known for these effects, but they are believed to average less than 10 kev. This number is estimated from the length of the yield pulse (0.5 microsecond) and from the over-all stability of the betatron. If energy jitter is significant (and we combine both the above possibilities under this heading), then the actual width of the cross section shown in Fig. 6 is less than 18 kev. An investigation of the effects of jitter was made using Gaussian curves of various widths as jitter functions. It was concluded that energy jitter is not important if the full width at half-maximum of the jitter function is less than about 15 kev.

The full width at half-maximum for the cross section was taken to be 18±5 kev.

The ordinates of all the yield curves obtained in this experiment are in arbitrary units. To obtain the peak cross section value of 1.4 millibarns shown in Fig. 6, the relative yield curve values of Fig. 1 were normalized to published curves. The Saskatchewan group has published two yield curves with absolute ordinates[1,2] and they do not agree with each other. The reason for this disagreement is not known.[14] The curve published by Montalbetti and Katz[2] does not agree with Fig. 1 in shape, whereas the curve of Horsley *et al.*[1] does. Furthermore, this latter curve agrees in shape with the curves published by Katz *et al.*[10] For these reasons, the curve given by Horsley[1] was used here. The absolute yield of the reaction at 20.33 Mev was taken to be $0.54\times 10^4$ neutrons per mole per roentgen.

If the cross section is assumed to have the shape of a Breit-Wigner resonance, the following expression can be written for the area under the resonance:

$$\int \sigma(E)dE = \tfrac{1}{2}\pi\Gamma\sigma_{\max}. \qquad (1)$$

In Eq. (1) the left-hand side represents the area under the resonance, $\Gamma$ is the full width of the resonance at half-maximum, and $\sigma_{\max}$ is the peak value of the cross section. The values of $\Gamma=18$ kev and $\sigma_{\max}=1.4$ mb have been established for the resonance causing the 16.03-Mev break. Inserting these into Eq. (1), we obtain $\int\sigma dE=0.040$ Mev-mb. This figure is lower than, but not in essential disagreement with an estimate of 0.06 Mev-mb made by Katz *et al.*[11]

### (b) Level Widths

The cross-section analysis just described gave the width of the resonance causing the 16.03-Mev break as 18 kev. Inspection of the breaks on all sections of the yield curve which were measured showed no apparent change in the general nature of the breaks, whether near threshold or on the giant resonance. Hence, one is tempted to state that they are all caused by levels of the same width, and that the width is of the order of 20 kev. Further support for this opinion was obtained from a series of yield curve calculations using thick target bremsstrahlung spectra and Breit-Wigner cross sections of various widths. It was concluded that levels as wide as 70 kev would not cause a sudden enough change in slope to be detected as a break, and that the observed breaks are so sudden that the level widths are less than 40 kev. For the purposes of further analysis, it was assumed that all the observed yield curve breaks are caused by levels of width 25 kev.

It should be noted that these considerations on level widths imply that levels of width greater than about 70 kev may lie beneath the levels observed in this experiment.

### (c) Integrated Cross Sections

By using the information obtained on the level causing the 16.03-Mev break, and the considerations on level widths given above, it was possible to obtain values for the integrated cross sections of the levels causing the observed breaks.

An estimate of the yield due to the level causing a given break is obtained by extrapolating the yield curve from energies below the break. Typical extrapolations are shown in all the detailed diagrams of the yield in this paper. The extrapolation was carried 93 kev past the energy of the break.

If it is assumed that $Y_i$ represents all the yield from the level in question, then one can write:

$$Y_i \propto \int_{E_b}^{E_b+\Delta} N(E_b+\Delta, E)\frac{\sigma_{\max}{}^i dE}{1+[2(E-E_i)/\Gamma]^2}, \qquad (2)$$

TABLE I. Summary of properties for observed levels of $O^{16}$.

| Energy of break (Mev) | $\int\sigma dE$ Mev-mb | $\sigma_{\max}$[a] (mb) | Radiation widths (ev) $J=2^+$ | $J=1^-$ |
|---|---|---|---|---|
| 15.85 | 0.0046 | 0.12 | 0.81 | 0.41 |
| 16.03 | 0.040 | 1.02 | 4.19 | 2.87 |
| 16.47 | 0.027 | 0.69 | 1.63 | 1.75 |
| 16.75 | 0.041 | 1.04 | 2.09 | 2.65 |
| 16.95 | 0.084 | 2.14 | 4.05 | 5.50 |
| 17.02 | 0.111 | 2.83 | 5.36 | 7.29 |
| 17.13 | 0.262 | 6.67 | 12.2 | 17.2 |
| 17.18 | 0.404 | 10.3 | 18.8 | 26.6 |
| 17.55 | 0.202 | 5.14 | 9.04 | 13.5 |
| 17.68 | 0.182 | 4.63 | 8.15 | 12.2 |
| 17.84 | 0.254 | 6.47 | 11.37 | 17.2 |
| 18.04 | 0.059 | 1.50 | 2.66 | 4.02 |
| 18.70 | 0.094 | 2.39 | 4.47 | 6.76 |
| 19.01 | 0.130 | 3.31 | 6.42 | 9.59 |
| 19.18 | 0.396 | 10.1 | 19.2 | 29.5 |
| 20.33 | 0.495 | 12.6 | 30.8 | 42.7 |
| 20.58 | 0.603 | 15.4 | 39.1 | 54.3 |
| 20.79 | 0.617 | 15.7 | 41.9 | 58.2 |
| 20.93 | 0.857 | 21.8 | 58.8 | 83.4 |
| 21.21 | 1.36 | 34.6 | 98.5 | 142.9 |
| 21.52 | 0.853 | 21.7 | 64.1 | 98.3 |
| 22.37 | 2.21 | 56.3 | ... | 322 |
| 22.54 | 3.14 | 80.0 | ... | 480 |
| 22.76 | 3.47 | 88.4 | ... | 549 |
| 23.02 | 3.06 | 77.9 | ... | 501 |

[a] $\sigma_{\max}$ was calculated using $\Gamma=25$ kev for all levels.

[14] L. Katz (private communication, May, 1955).

where $E_b$ is the energy of the break, $E$ is the photon energy, $E_i$ is the resonance energy, $\Gamma$ is the width of the resonance, $\sigma_{max}{}^i$ is the peak value of the cross section, and $N(E_b+\Delta, E)$ is the bremsstrahlung spectrum.

Calculations with test cross sections have shown that the observed position of the break comes about the width of the level below the resonance energy. Hence

$$E_i = E_b + \Gamma. \qquad (3)$$

The bremsstrahlung spectrum which is used in Eq. (2) must be a thick target spectrum, since we are only interested in the first 93 kev from the high-energy tip. The spectrum can be well represented by the equation:

$$N(E_b+\Delta, E) = \frac{\Phi(E_b+\Delta-E)}{[E_b+\Delta][0.1(E_b+\Delta)+0.26]}, \qquad (4)$$

where $\Phi$ is a function whose value depends only on the energy difference between $E$ and the maximum energy, and the term $[0.1(E_b+\Delta)+0.26]$ takes into account the energy dependence of the monitor response.

If the results of Eqs. (2), (3), and (4) are combined and a simple transformation of variables is made, the following equation results:

$$Y_i \propto \frac{\Gamma\sigma_{max}{}^i}{[E_b+\Delta][0.1(E_b+\Delta)+0.26]} \times \int_{-2}^{(2\Delta/\Gamma)-2} \frac{\Phi(\Delta-\Gamma-\Gamma x/2)}{1+x^2} dx. \qquad (5)$$

There are two conditions for which the integral in Eq. (5) has a constant or near constant value. These are if $\Gamma$ is constant, or if $\Delta$ is much greater than $\Gamma$. For the present analysis the integral was assumed to be constant with value $K$.

From Eq. (1), $\Gamma\sigma_{max}{}^i$ is proportional to the integrated

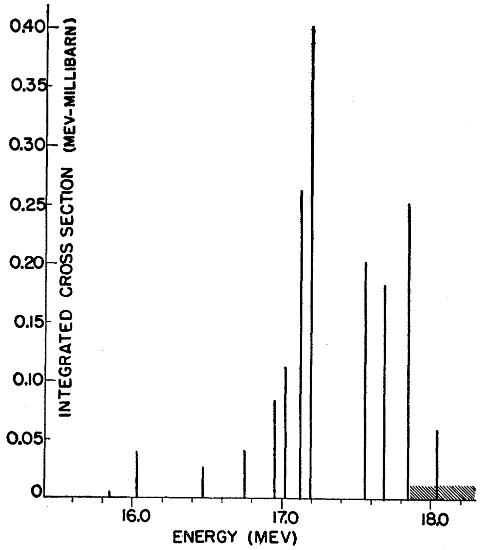


FIG. 7. Integrated cross sections for levels between threshold and 18 Mev.

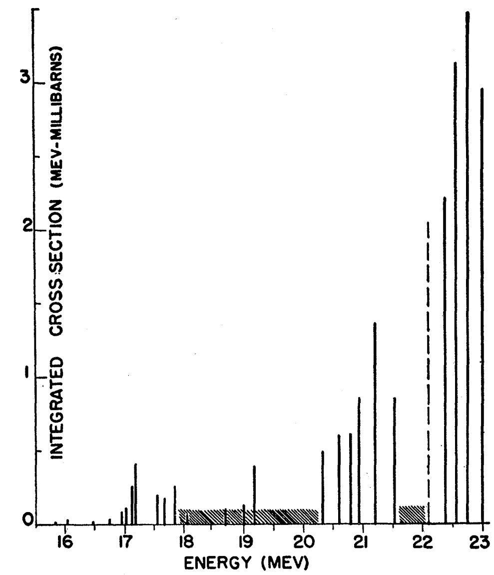


FIG. 8. Integrated cross sections of all levels found in this work.

cross section for the level, and therefore

$$Y_i = K_1 \frac{\int \sigma(E)dE}{[E_b+\Delta][0.1(E_b+\Delta)+0.26]}. \qquad (6)$$

The constant of proportionality, $K_1$, was evaluated from the information obtained on the 16.03-Mev break. Then, using Eq. (6) the integrated cross sections for all the observed levels were computed. The results are shown in Table I, and in Figs. 7 and 8.

The shading in Figs. 7 and 8 indicates regions in which the yield was not measured carefully, or not measured at all. The integrated cross section values should be accurate to within about 25%.

If 3 Mev-millibarns is allowed for the integrated cross section contained in the regions which were not covered at all (i.e., 19.2 to 20.3 Mev and 21.5 to 22.1 Mev), then the total integrated cross section to 23.2 Mev is found to be 22 Mev-millibarns. This value compares favorably with previously published figures of 31 Mev-millibarns to 24 Mev,[1] 14 Mev-millibarns to 22 Mev,[2] and 31 Mev-millibarns to 25 Mev.[3] These values were obtained from a gross cross-section analysis, and must include the integrated cross section of the levels detected in this experiment, the integrated cross section of any levels that were missed, and the contribution from a possible continuum cross section.

The figure of 23 Mev-millibarns given by the present experiment seems to account for the total integrated cross section. Hence one can conclude that the bulk of the $(\gamma,n)$ reaction occurs in narrow levels.

### (d) Peak Heights of the Levels

By using the integrated cross sections for the individual levels which have been derived, the value of 25 kev assumed for the widths of all the levels, and Eq. (1), the peak heights of the levels may be computed. The results are given in Table I.

If one assumes that protons as well as neutrons are emitted from the observed levels, it can be estimated (see the next section) that on the average 1.5 times as many protons as neutrons are emitted from the levels. Hence an estimate of the peak gamma-ray absorption cross section can be obtained by multiplying the peak cross sections obtained by 2.5. A figure of 180 millibarns is obtained for peak values on the giant resonance.

### (e) Radiation Widths

The radiation width of a level is related to its integrated cross section by the formula:

$$\int \sigma(E)dE = \frac{7.7S_0\Gamma_\gamma}{E_i^2}G_n, \qquad (7)$$

where $E_i$ is the energy of the level in Mev, $\Gamma_\gamma$ is the radiation width in ev, $S_0$ is a statistical factor, and $G_n$ is the branching ratio for neutrons. It should be noted that Eq. (7) is independent of the level width $\Gamma$.

The statistical factor, $S_0$, is equal to $(2J+1)/2(2I+1)$, where $J$ is the spin of the compound nucleus and $I$ is the spin of the ground state of the target nucleus. Since the ground state of $O^{16}$ has spin $0^+$, $S_0$ is 3/2 for dipole transitions and 5/2 for quadrupole transitions.

The branching ratio, $G_n$, is equal to the partial width for neutron emission divided by the total width of the states, and the total width is the sum of the partial widths for decay by emission of neutrons, protons, alpha particles, and radiation.

The partial width for radiative decay should be small compared to the partial width for particle emission, so it is neglected. Using the results of Spicer[15] on the $(\gamma,p)$ reaction in $O^{16}$, and the results of Nabholz, Stoll, and Waffler[16] on the $(\gamma,\alpha)$ reaction, one concludes that alpha-particle emission may be neglected, since $\Gamma_\alpha/\Gamma_p$ is about 0.1 over most of the region covered. The total level width was therefore taken to be the sum of the partial widths for neutron and proton emission. Thus:

$$G_n(E_i) = \Gamma_n(E_i)/[\Gamma_n(E_i)+\Gamma_p(E_i)]. \qquad (8)$$

In general there will be several ways in which the compound state can decay by neutron or proton emission. $\Gamma_n$ and $\Gamma_p$ will consist of a sum over the various open channels. The relative magnitudes of the terms in this sum are conditioned by many factors including the spin of the compound state, the angular momentum carried off by the particle, and the spin and parity of the residual state.

By using Blatt and Weisskopf[17] as a reference, the following formula was obtained:

$$\Gamma_n(E_i) = \sum_i \mathcal{S}(J,s,i) \sum_S \sum_l \omega_l(\Pi_i,\Pi_J)T_{nl} \times(\epsilon_n)\gamma_n(JlSi), \qquad (9)$$

where $J$ is the spin of the compound $O^{16}$ state, $i$ is the spin of the residual state in $O^{15}$, $S$ is the channel spin (with values of $i\pm\frac{1}{2}$), $l$ is the angular momentum of the emitted particle, $\Pi$ designates the parity quantum number, and $s$ is the spin of the neutron.

A similar expression holds for $\Gamma_p(E_i)$.

$\mathcal{S}$ is a statistical factor which has the value of $(2J+1)/(2s+1)(2i+1)$, $\omega_l(\Pi_i,\Pi_J)$ is a function which guarantees parity conservation since it has nonzero value only if $\Pi_J=(-1)^l\Pi_i$, $T_{nl}(\epsilon_n)$ is the barrier penetration factor for neutrons of energy $\epsilon_n$ and angular momentum $l$, and $\gamma_n(JlSi)$ is the reduced width for decay into the channel specified by the quantum numbers $J$, $l$, $S$, $i$.

Nothing is known about the reduced widths $\gamma_n$—either of their energy dependence or their dependence on the specified quantum numbers. They describe the frequency with which a proton or neutron appears at the nuclear surface with the right angular momentum, spin direction, and energy while the remainder of the nucleus is in the proper configuration to form the residual state. Their calculation requires the adoption of a nuclear model.

For the present analysis the *ad hoc* assumption was made that all the $\gamma$ are equal in value for a given energy of the compound nucleus. Then they cancel out of Eq. (8).

The barrier penetration factors for neutrons were obtained from Blatt and Weisskopf[18] and for protons from Feshback, Shapiro, and Weisskopf.[19] In making the calculations the nuclear radius was taken to be $1.50\times10^{-13}A^{\frac{1}{3}}$, and the inside wave number was taken to be $10^{13}$ cm$^{-1}$.

The spins and parities of the residual states in $O^{15}$ and $N^{15}$ were obtained from the review article of Ajzenberg and Lauritsen.[7] In some cases two alternate values were given for the spins. Then $G_n$ was computed for both of them and an average value was taken (in most cases the difference was less than 10%).

Values of $G_n$ were computed for the two cases $J=1^-$ and $J=2^+$, corresponding to electric dipole and electric quadrupole transitions. $\Gamma_p/\Gamma_n$ was found to be roughly 1.5 over most of the energy region covered for both choices of $J$. It is presumably also true for $J=1^+$ which corresponds to magnetic dipole transitions.

Using Eq. (7), the calculated values of $G_n$, and the values for the integrated cross sections which have been obtained, radiation widths were calculated for assumed $J$- values of $1^-$ and $2^+$. The results are given in Table I.

The calculated values are not greatly dependent on

[15] B. M. Spicer, Phys. Rev. **99**, 33 (1955).
[16] Nabholz, Stoll, and Waffler, Phys. Rev. **86**, 1043 (1952).
[17] J. M. Blatt and V. F. Weisskopf, *Theoretical Nuclear Physics* (John Wiley and Sons, Inc., New York, 1948), Chap. 8.
[18] Reference 17, p. 361.
[19] Feshbach, Shapiro, and Weisskopf, Nuclear Development Associates Report NYO 3077, 1953 (unpublished).

the assumed value for $J$. The difference for the two $J$-values is often less than 25%.

There is a wide variation in the calculated widths. They rise from a few electron volts near threshold to about 500 electron volts at 23 Mev.

In order to try to identify the type of transitions one would like to compare the calculated widths to experimental measurements for $E1$, $M1$, and $E2$ transitions. This was possible for the former two types, but not for the latter. There is little experimental information on $E2$ widths so the present results were compared to a theoretical $E2$ curve.

A survey of experimental $E1$ and $M1$ radiation widths has been given by Wilkinson[20] for light nuclei, and by Kinsey and Bartholemew[21] for medium weight nuclei. The conclusions from the two surveys are in fairly good agreement. Wilkinson gives the following formulas:

$$\Gamma_\gamma(E1)=[0.022/(2J+1)]A^{\frac{2}{3}}E_i^3, \qquad (10)$$

$$\Gamma_\gamma(M1)=0.003E_i^3. \qquad (11)$$

Kinsey and Bartholomew[21] conclude that observed $E2$ radiation widths fluctuate considerably, and may be much higher or much lower than the theoretical estimates of Weisskopf.[22] Since there are no firm experimental conclusions for $E2$ transitions, the present results were compared to the theoretical estimates of Weisskopf. The formula for $O^{16}$ is:

$$\Gamma_\gamma(E2)=6.3\times10^{-6}E_i^5 \text{ (ev)}. \qquad (12)$$

The comparison of the calculated widths with the predictions of formulas (10) and (12) is made in Table II.

On the basis of this comparison, one concludes that the levels between threshold (15.6 Mev) and 19 Mev have radiation widths which are far too small for them to be electric dipole. These levels must then be reached by either magnetic dipole or electric quadrupole transitions. Since a magnetic dipole transition requires an angular momentum change of $\pm1$ or 0 and no parity change the shell model predicts no $M1$ transitions for $O^{16}$. This is because the $1p$ shell fills at $O^{16}$. On this basis one might guess that the levels between threshold and 19 Mev are reached by $E2$ transitions. This has been confirmed by Spicer[15] in a study of the angular distribution of protons in the $(\gamma,p)$ reaction at and near the $(\gamma,n)$ threshold.

The group of levels between 22 and 23 Mev have radiation widths which are almost as large as those predicted by Wilkinson's equation.[20] These levels are likely reached by $E1$ transitions. It should be noted, however, that Wilkinson's equation is based on observed $E1$ transitions at about 13 Mev and less and there is some question about extrapolating it to energies as high as 23 Mev. This doubt is increased when one considers that the equation predicts a monotonic increase in the widths as the energy is raised, while photonuclear cross sections exhibit a giant resonance which is believed to be dipole in character. One might argue that the giant resonance is caused by a sharp increase in the density of $1^-$ states and not by a "resonance" in the strength of the radiative widths. This argument is contrary to all theoretical predictions on level densities and is contrary to the approximately constant density observed in the present experiment as well, In any case, the levels between 22 and 23 Mev come up to Wilkinson's estimate, and they lie on the peak of the giant resonance.

TABLE II. Radiation widths.

| Break energy (Mev) | $\int\sigma dE$ (Mev-mb) | Radiation widths: $E2$ absorption $J=2^+$ Observed | Weisskopf | $E1$ absorption $J=1^-$ Observed | Wilkinson |
|---|---|---|---|---|---|
| 15.85 | 0.0046 | 0.81 | 6.3 | 0.41 | 186 |
| 16.03 | 0.040 | 4.19 | 6.7 | 2.87 | 193 |
| 16.47 | 0.027 | 1.63 | 7.6 | 1.75 | 208 |
| 16.75 | 0.041 | 2.09 | 8.3 | 2.65 | 219 |
| 16.95 | 0.084 | 4.05 | 8.7 | 5.50 | 227 |
| 17.02 | 0.111 | 5.36 | 8.9 | 7.29 | 230 |
| 17.13 | 0.262 | 12.2 | 9.2 | 17.2 | 234 |
| 17.18 | 0.404 | 18.8 | 9.3 | 26.6 | 236 |
| 17.55 | 0.202 | 9.04 | 10.2 | 13.5 | 252 |
| 17.68 | 0.182 | 8.15 | 10.7 | 12.2 | 257 |
| 17.84 | 0.254 | 11.4 | 11.1 | 17.2 | 265 |
| 18.04 | 0.059 | 2.66 | 11.8 | 4.02 | 274 |
| 18.70 | 0.094 | 4.47 | 14.1 | 6.76 | 305 |
| 19.01 | 0.130 | 6.42 | 15.5 | 9.59 | 320 |
| 19.18 | 0.396 | 19.2 | 16.2 | 29.5 | 329 |
| 20.33 | 0.495 | 30.8 | 21.6 | 42.7 | 392 |
| 20.58 | 0.603 | 39.1 | 23.0 | 54.3 | 406 |
| 20.79 | 0.617 | 41.9 | 24.1 | 58.2 | 419 |
| 20.93 | 0.857 | 58.8 | 25.0 | 83.4 | 427 |
| 21.21 | 1.36 | 98.5 | 26.9 | 142.9 | 444 |
| 21.52 | 0.853 | 64.1 | 29.0 | 98.3 | 464 |
| 22.37 | 2.21 | ... | 36.0 | 322.1 | 521 |
| 22.54 | 3.14 | ... | 37.0 | 479.6 | 533 |
| 22.76 | 3.47 | ... | 38.6 | 549.1 | 549 |
| 23.02 | 3.06 | ... | 41.0 | 501.4 | 568 |

The levels between 20 and 21.5 Mev have radiation widths 2 to 4 times larger than the $E2$ prediction and 1/5 to 1/10 of the $E1$ prediction. It is completely uncertain which class they should be placed in. The surveys of $E1$ widths[20,21] show variations of about a factor of 6 from Eq. (10) so that they may be $E1$. There is an $E1$ transition in $O^{16}$ at 13.09 Mev and its radiative width is 150 ev. This is about 70% of the value predicted by Eq. (10).

### (f) Cross Section at 17.63 Mev

Measurements of the $O^{16}(\gamma,n)O^{15}$ cross section at an energy of 17.63 Mev have been made with gamma rays from the $Li^7(p,\gamma)Be^8$ reaction. Waffler and Younis[23] obtained a value of $0.54\pm0.14$ millibarn, and Walker *et al.*[24] obtained a value of $1.3\pm0.3$ millibarns. The

[20] D. H. Wilkinson, Phil. Mag. 44, 450, 1019 (1953).
[21] B. B. Kinsey and G. A. Bartholomew, Phys. Rev. 93, 1260 (1954).
[22] V. F. Weisskopf, Phys. Rev. 83, 1073 (1951).
[23] H. Waffler and S. Younis, Helv. Phys. Acta 22, 614 (1949).
[24] Walker, McDaniel, and Stearns, Phys. Rev. 80, 807 (1950).

latter authors did their measurement using a thick lithium target whereas the former do not state their target thickness.

Using the results of the present experiment, a value for the cross section at 17.63 Mev was obtained. This value would correspond to an experimental measurement made with a thin Li target. The energy 17.63 Mev falls between two resonance levels, and so the cross section at that energy is obtained by summing the contributions from the tails of the neighboring levels. Since there is doubt as to the proper value to use for the level widths, computations were done for widths of 20 and 30 kev. The results were 0.29 mb for $\Gamma=20$ kev, and 0.42 mb for $\Gamma=30$ kev. These are lower than the experimental results, but not in essential disagreement, especially when one considers that the use of a thick lithium target would tend to increase the measured values, since the 17.68-Mev level would contribute more than has been allowed for in the calculation.

This agreement gives additional evidence for the conclusion that absorption of gamma-rays by the $O^{16}$ nucleus takes place chiefly into narrow levels since all of the cross section at 17.63 Mev can be accounted for by the contributions from the tails of the levels near this energy.

## SUMMARY

A careful survey of the $O^{16}(\gamma,n)O^{15}$ yield curve has been made over a large portion of the energy region between 15.6 Mev and 23.2 Mev. Fine structure, in the form of sudden changes in slope, was observed. The existence of these breaks has been reported by Katz *et al.*[10] and the present experiment is the first independent confirmation.

Points on the yield curve were obtained every 10 to 15 kev over most of the region covered whereas the Saskatchewan group measured every 30 to 60 kev. As a result of the more detailed nature of the present work many more breaks were resolved. This is particularly true of the 20- to 23-Mev region, where scallop-like breaks were observed while Katz *et al.*[10] observed two breaks with straight line segments in between.

An average frequency of 5 breaks per Mev, was observed over all of the energy region covered.

The breaks were interpreted as manifestations of narrow resonances in the $(\gamma,n)$ cross section. This interpretation was substantiated by the concave-down nature of the yield curve between breaks, and by a detailed cross section analysis of one of the breaks.

The radiative widths which were obtained indicate that up to 19 Mev, the levels are reached by $E2$ transitions, where as between 22 and 23 Mev the transitions are most likely $E1$. It was impossible to decide the nature of a group of levels between 20 and 21 Mev, since the observed radiative widths were intermediate between the predictions for $E1$ and $E2$ absorption.

The ability to resolve breaks (considering only statistical fluctuations in the activity measurements) was investigated by a Monte Carlo method. It is felt that, by following the procedure described, breaks 50 or 60 kev apart can be resolved, providing that the second one is at least as strong as the first.

It is difficult to quote a figure for the probable error to be assigned to the calculated integrated cross sections, peak heights, and radiative widths. The figures given below are estimates.

*Integrated cross sections.*—The relative values are good to $\pm 15\%$ and the chief source of error is the counting statistics, and the making of the necessary extrapolation. The absolute values are good to $\pm 25\%$.

*Peak heights.*—These are good to $\pm 50\%$. The increase in the quoted error over that for the integrated cross sections is due to the uncertainty in the level widths.

*Rddiative widths.*—The chief sources of error are the counting statistics and the assumptions which were made in computing the branching ratio for neutrons. The radiative widths are estimated to be accurate to $\pm 35\%$.

*Energy of the levels.*—It is estimated that the relative positions of the breaks are good to $\pm 15$ kev, and so the break energies were quoted to the nearest 10 kev. It was pointed out that the level should be located above the break position by the width of the level. Since the level widths are not known exactly, this adds an additional 10 to 15 kev to the uncertainty. On top of this one must consider the uncertainty in the absolute energy calibration of the betatron. The possible error in the absolute calibration is taken to be $\pm 30$ kev up to 18 Mev with a gradual increase to $\pm$ 300 kev at 23 Mev. These comments on the calibration assume that the observed oxygen and carbon thresholds correspond to thresholds which would be computed from mass measurements. Hence, though the relative positions are rather well determined, the absolute positions are poorly determined.

The cross section at 17.63 Mev was computed, assuming that all of the cross section was contributed from the tails of the neighbouring levels. Agreement was found with a measurement by Waffler and Younis[23] using the Li $\gamma$-rays. This agreement, and the fact that the sum of the integrated cross sections of the levels can account for all of the integrated cross section (as determined by gross analyses of the yield curve) indicates that at least the bulk of the photon absoprtion takes place into narrow levels.

## ACKNOWLEDGMENTS

Thanks are due to Professor A. O. Hanson for many helpful discussions, and to Professor L. Katz, of the University of Saskatchewan, for stimulating discussions and correspondence. The authors wish to record their indebtedness to Mr. T. J. Keegan and the operating crew of the 22-Mev betatron who did a splendid job of maintaining and operating the betatron.